Synthesis of Functional Polymer Brushes Containing Carbohydrate Residues in the Pyranose Form and Their Specific and Nonspecific Interactions with Proteins

Kai Yu[†] and Jayachandran N. Kizhakkedathu*[,†,‡]

Centre for Blood Research and Department of Pathology & Laboratory Medicine, and Department of Chemistry, University of British Columbia, Vancouver, British Columbia V6T 1Z3, Canada

Received July 30, 2010; Revised Manuscript Received September 14, 2010

Three novel N-substituted acrylamide monomers containing different carbohydrate residues, 2′-acrylamidoethyl-α-D-mannopyranoside, 2′-acrylamidoethyl-β-D-glucopyranoside, and 2′-acrylamidoethyl-β-D-galactopyranoside, in the pyranose form were synthesized. The corresponding glycopolymer brushes were prepared on silicon substrates by surface-initiated atom transfer radical polymerization (SI-ATRP) using unprotected glycomonomers. The formation of glycopolymer brushes was well-characterized using ellipsometry, ATR-FTIR, water contact angle analysis, atomic force microscopy analysis, and X-ray photoelectron spectroscopy. The effects of halogen, ligand, and solvent on the polymerization were thoroughly investigated. It was shown that CuCl/$CuCl_2$/tris(2-dimethylaminoethyl)amine (Me_6TREN) catalytic system with an optimized ratio of Cu(I)/Cu(II) produced glycopolymer with high molecular weight ($M_n = 44-140$ kDa) and relatively narrow molecular weight distribution (PDI = 1.4). The dry thickness of resulting glycopolymer brushes (10−36 nm) showed a proportional relationship with the molecular weight of free polymer generated in the solution. The grafting densities of obtained glycopolymer brushes were between 0.12 and 0.17 chains/nm^2. The grafting of glycopolymer resulted in highly hydrophilic surface layer with very low water contact angles (<10°). The glycopolymer brushes showed ultralow protein adsorption from bovine serum albumin (BSA) and fibrinogen (Fb) solutions. Glycopolymer brushes containing glucose units showed relatively better protection against BSA and Fb adsorption than those brushes containing mannose and galactose units. Synthesized glycopolymer brushes retained specific protein interactions, as evident from the interaction with Concanavalin A (Con A). The interaction of surface-grafted glycopolymer brushes with Con A depended on both the stereochemistry of carbohydrate units and the chemical structures present. In addition, the newly synthesized glycopolymer brushes performed significantly better in comparison with currently available structures in terms of specific protein interactions.

Introduction

The glycocalyx is a "carbohydrate-rich coat" on the external surface of the plasma membrane of cells. The interactions of glycocalyx with proteins present in the surrounding environments are important recognition events that regulate a myriad of biological and pathological processes, including cell recognition,[1,2] viral infection,[3] and cancer metastasis.[4] The carbohydrate groups participate in these processes through the specific interaction with their partner proteins with high specificities. In addition, the glycocalyx also serves as a layer that prevents the undesirable nonspecific adhesion of other proteins and cells.[5−8] Therefore, preparation of artificial cell surface by mimicking of the glycocalyx may provide a promising route not only for comprehensive understanding of carbohydrate-receptor interactions but also for the development of highly biocompatible surfaces.

The glycocalyx-mimetic surfaces prepared by the physical adsorption showed efficient reorganization with receptor[9,10] and good nonfouling properties.[11−14] Although this physical attachment method gave useful properties, the low sugar density, instability, and random orientation of sugars might not reflect their natural presentation in living systems, which decreases the efficiency of reorganization. Covalent grafting of monosaccharide or oligosaccharide by direct grafting ("grafting to" or "grafting from") techniques, can potentially overcome these shortcomings. These techniques include the formation of a self-assembled monolayer (SAM),[15,16] covalent immobilization of modified carbohydrates directly onto functionalized glass or silicon slides,[17−19] activated ester-derivatized surface,[20,21] and the use of "click chemistry".[22,23] However, most of these methods suffer from drawbacks such as stability under various conditions, limitation of the range of immobilized carbohydrate, and the substrate-dependent nature of specific covalent attachment chemistry.[24]

Despite the fact that carbohydrate−protein interaction has shown high specificity, the affinity between the proteins and simple sugar residues is low ($K_a = 10^3-10^4$ L·mol^{-1}) because of the monovalent interaction.[25,26] A multivalent presentation of ligands is generally required to achieve physiologically relevant association and affinities. Grafting glycopolymer chains onto surface with high grafting density (keeping the glycopolymer chains highly stretched state) may be a good scaffold to mimic the glycocalyx and may provide a means to study the carbohydrate−protein interactions. To achieve this objective, Ejaz and Fukuda were the first to report the preparation of glycopolymer brushes using surface-initiated atom transfer radical polymerization (SI-ATRP) of a methacrylate-based acetate-protected glucose-containing monomer,[27] followed by the deprotection to gain the sugar functionalities.[28] Similar

* To whom correspondence should be addressed: E-mail: jay@pathology.ubc.ca. Tel: (604) 822-7085.
[†] Centre for Blood Research and Department of Pathology & Laboratory Medicine.
[‡] Department of Chemistry.

10.1021/bm100882q
Published on Web 10/18/2010

approaches were then reported by Müller and coworkers for the preparation of glycopolymer brush on carbon nanotubes and Si wafer.[29,30] By using a sugar-containing monomer D-gluconamidoethyl methacrylate (GAMA),[31] Yang and Xu successfully prepared linear and comb-like grafted glycopolymer layers on polypropylene membranes using SI-ATRP without the deprotection step.[32,33] It was shown that poly(D-gluconamidoethyl methacrylate) (PGAMA) brushes exhibited promising resistance to nonspecific adsorption of proteins, including BSA, lysozyme, and fibrinogen (Fb).[34,35] Although the glycopolymer surfaces produced by these methods showed good reduction in nonspecific protein adsorption, the specific protein interaction was compromised. This is due to the fact that none of the glycopolymer brushes reported have sugar residues in the pyranose form, and in some cases, the core carbohydrate structure is modified or in the open form.[28−35] It is important that sugar residues should be in the pyranose form as found on the cell surface[36] and the differences in sugar structures and stereochemistry may have influence in both specific and nonspecific interactions with proteins.[36,37] An exception to this is a recent report by Mateescu et al., who used poly(2-lactobionamidoethyl methacrylate) brushes that exhibited considerable binding interactions with galactose-binding lectin via the "glycocluster" effect.[38] Unfortunately, only the galactose-functionalized polymer layer can be prepared by this method, and variation of carbohydrate structure is not possible.

Another important disadvantage in the synthesis of glycopolymer brushes using post-deprotection procedure is the difficulty in quantitative removal of protecting groups on sugar moieties. Incomplete deprotection of sugar residues might impact the biological properties of sugar unit and may introduce hydrophobic patches on the surface as well. These hydrophobic binding sites may attract certain proteins to the surface, especially in complex biological fluids. Therefore, it is critical to develop methods for the synthesis of glyco-polymer surfaces bearing carbohydrate units having similar stereochemistry to that present on cell surface glycocalyx to investigate their role in both specific interactions and nonspecific interactions in biological environments. Therefore, in the present work, we report the synthesis of three novel hydrolytically stable, N-substituted acrylamide monomers carrying mannose, galactose, and glucose in the pyranose form and the preparation of glycopolymer brushes using these monomers without post-deprotection procedure. A preliminary study on nonspecific and specific interactions between glycopolymer brushes and proteins was also carried out to illustrate the dependence of these interactions on sugar structures and stereochemistry. We also synthesized previously reported glycopolymer brushes and compared them with the newly developed carbohydrate brushes.

Experimental Section

Materials. D-(+)-Mannose (99%) was purchased from Alfa Aesar (Heysham, Lancashire, England) and used as received. β-D-Glucose pentaacetate (98%), β-D-galactose pentaacetate (98%), boron trifluoride diethyl etherate (purified by redistillation), 2-bromoethanol (95%), palladium on carbon (10 wt % loading), acryloyl chloride (97%), sodium methoxide solution (25 wt % in methanol), copper(I) chloride, copper(II) chloride, tris(2-aminoethyl)amine, 2-chloropropionyl chloride (97%), methyl 2-chloropropionate (97%), trichlorosilane (99%), and albumin-fluorescein isothiocyanate conjugate (bovine serum albumin, product number: A9771) were purchased from Sigma-Aldrich (Oakville, ON). Karstedt catalyst (platinum-divinyltetramethyl-disiloxane complex in xylene 2.1 to 2.4% Pt) was purchased from Gelest (Morrisville, PA). 1-Amino-10-undecene (97%) was purchased from GFS chemicals (Columbus, Ohio). Fb (from human plasma), Alex-fluor 594 conjugate (product number: F13193), and tetramethylrhodamine conjugates of concanavalin A (Con A, product number: C860) were purchased from Invitrogen. (Eugene, Oregon). 2-Azidoethanol was prepared from 2-bromoethanol and sodium azide in the presence of sodium hydroxide.[39] ^{1}H NMR (300 MHz, $CDCl_3$): 3.42−3.45 (t, 2H), 3.75−3.79 (t, 2H) ppm. Tris[2-(dimethylamino)ethyl]amine (Me_6TREN) was prepared by the previously reported procedure.[40] ^{1}H NMR (300 MHz, $CDCl_3$): 2.25 (s, 18H), 2.38−2.43 (t, 6H), 2.6−2.63 (t, 6H) ppm. Ester derivative of surface ATRP initiator (11-(2-bromo-2-methyl)-propionyloxy)-undecyl-trichlorosilane) was synthesized by the use of a similar procedure reported in the literature.[41] ^{1}H NMR (300 MHz, $CDCl_3$): 1.28−1.42 (br m, 16H), 1.55−1.70 (m, 4H), 1.93 (s, 6H), 4.15−4.19 (t, 2H) ppm.

Characterization. NMR spectra were recorded on a Bruker Avance 300 MHz NMR spectrometer using deuterated solvents (Cambridge Isotope Laboratories, 99.8% D) with the solvent peak as a reference. Molecular weights and polydispersities of glycopolymer samples were determined using gel permeation chromatography (GPC) on a Waters 2690 separation module fitted with a DAWN EOS multiangle laser light scattering (MALLS) detector from Wyatt Technology. with 18 detectors placed at different angles and a refractive index detector (Optilab DSP from Wyatt Technology). An Ultrahydrogel linear column with bead size 6−13 μm (elution range 10^3 to 5×10^6 Da) and an Ultrahydrogel 120 with bead size 6 μm (elution range 150 to 5×10^3 Da) from Waters were used. The d*n*/d*c* value of glycopolymer carrying mannose residues in the mobile phase was determined at $\lambda = 620$ nm to be 0.154 mL/g and was used for determining molecular weight parameters. The d*n*/d*c* values are 0.158, 0.159, 0.148, and 0.15, respectively, for poly(2′-acrylamidoethyl-β-D-galactopyranoside) (PAAEGal), poly(2′-acrylamidoethyl-β-D-glucopyranoside) (PAAEGlc), PGAMA, and poly(3-*O*-methacryloyl-D-glucofuranose) (PMAGlc). Mass spectra were recorded on a Bruker Esquire electrospray (ESI) ion-trap instrument using samples dissolved in MeOH or water, with positive-ion polarity.

ATR-FTIR absorption spectra were collected on a Nexus 670 FT-IR ESP (Nicolet Instrument, Waltham, MA) with an MCT/A liquid nitrogen cooled detector, a KBr beam splitter, and an MkII Auen Gate single-reflection attenuated total reflectance (ATR) accessory (Specac, Woodstock, GA). Spectra were recorded at 4 cm^{-1} resolution, and 128 scans were collected. Initiator-modified silicon wafer was chosen as the background.

Water Contact Angle Measurements. A water droplet (6 uL) was placed on the surface, and an image of the droplet was taken with a digital camera (Retiga 1300, Q-imaging). The contact angle was analyzed using Northern Eclipse software. Over three different sites were tested for each sample.

XPS Measurement. X-ray photoelectron spectroscopy (XPS) was performed using a Leybold LH Max 200 surface analysis system (Leybold, Cologne, Germany) equipped with a Mg Kα source at a power of 200 W. Elements were identified from survey spectra. High-resolution spectra were collected at 48 eV pass energy.

The variable-angle spectroscopic ellipsometry (VASE) spectra were collected on an M-2000 V spectroscopic ellipsometer (J.A. Woollam, Lincoln, NE) at 55, 65, and 75° at wavelengths from 480 to 700 nm with an M-2000 50W quartz tungsten halogen light source. The VASE spectra were then fitted with a multilayer model utilizing WVASE32 analysis software based on the optical properties of a generalized Cauchy layer to obtain the "dry" thickness of the glycopolymer layers.

AFM Measurements. Atomic force microscopy measurements were performed on a multimode, Nanoscope IIIa controller (Digital Instruments, Santa Barbara, CA) equipped with an atomic head of 100 × 100 μm^2 scan range. The tapping mode was used to map the film morphology under ambient conditions. Silicon tips with a spring constant of 42 N/m and a frequency of 320 kHz were used. Root-mean-square (rms) roughness was evaluated using the integrated

software. The roughness was defined as the rms of height deviations taken from the mean data plane.

Deposition of ATRP Initiator on Si Wafer. We prepared the initiator layer by placing the Si wafer (1 cm ×1 cm) cleaned with Piranha solution (H_2O_2/H_2SO_4 3:7 (v/v) (*Piranha solution is an extremely strong oxidant and should be handled very carefully!*) in an anhydrous initiator solution in toluene (10 μL in 10 mL). The deposition time for amide derivatives of surface initiator was 20 min, whereas the deposition time for ester derivatives of surface initiator was 20 h. The initiator-modified Si wafer was then thoroughly rinsed sequentially with toluene, acetone, and anhydrous ethanol, followed by drying in nitrogen. The initiator-modified surface was characterized by contact angle measurements, ellipsometry measurements, and XPS analysis.

Synthesis of Monomers. *a. Synthesis of 1,2,3,4,6-penta-O-acetyl-D-mannose (***1***).* D-Mannose (25 g, 0.14 mol) and DMAP (2.5 g, 0.02 mol) were dissolved in anhydrous pyridine (200 mL) and cooled to 0 °C in an ice bath. Acetic anhydride (87.5 mL, 0.96 mol) was added dropwise to the solution. The mixture was allowed to stir at room temperature overnight. After completion of the reaction (followed by TLC), the mixture was poured in ice water with vigorous stirring and extracted with ethyl acetate. The extracts were subsequently washed with cold water, saturated aqueous sodium bicarbonate, and water until the pH reached ~7. The organic layer was dried over anhydrous sodium sulfate and evaporated in a rotary evaporator. The crude product was purified by flash column chromatography using ethyl acetate/hexane (1:1, v/v) to give compound **1** (44.6 g, 82.2% yield, α/β 4:1, $R_f = 0.39$, a colorless oil). ^{1}H NMR: (300 mHz, $CDCl_3$, δ): 2.01, 2.06, 2.10, 2.17, 2.18 (15H, s, Me); 4.04−4.08 (1H, m, H5); 4.12−4.17 (1H, dd, $J = 2.3$, 11.96 Hz); 4.26−4.31 (1H, dd, $J = 4.8$, 12.32 Hz, H6); 5.25−5.36 (3H, m, H2, 3, 4); 5.86 (1H, d, $J = 1.02$ Hz, H1β); 6.06 (1H, d, $J = 1.8$ Hz, H1α). ^{13}C NMR: (75.5 mHz, $CDCl_3$, δ): 20.69, 20.7, 20.75, 20.81, 20.90 (5C, CH_3); 62.15, 65.59, 68.40, 68.81, 70.67 (5C, C2, 3, 4, 5, 6); 90.49, 90.66 (1C, C1); 168.10, 169.57, 169.77, 170.01, 170.65 (5C, C═O). LR-MS (ESI): Calcd for $C_{16}H_{22}O_{11}Na$ $[M+Na]^+$, 413.33; found, 413.2.

*b. Synthesis of 2′-Azidoethyl-2,3,4,6-tetra-O-acetyl-α-D-mannopyranoside (***2***).* Compound **1** (20 g, 0.05 mol) was dissolved in 100 mL of anhydrous dichloromethane, and azidoethanol (7.1 g, 0.08 mol) was added via syringe. The resulting solution was stirred under argon and cooled to 0 °C. $BF_3 \cdot Et_2O$ (33 mL, 0.27 mmol) was then added dropwise. The reaction was stirred at 0 °C for 1 h and an additional 48 h at RT. After dilution with dichloromethane, the reaction mixture was washed with water, aqueous sodium carbonate, and cold water until pH ~7. The organic phase was dried over anhydrous sodium sulfate and evaporated in a rotary evaporator. Flash chromatography on silica gel (ethyl acetate/hexane 1:1) gives the title compound **2** as a crystalline solid in 76% yield as pure α anomer. ^{1}H NMR: (300 mHz, $CDCl_3$, δ): 2.0, 2.06, 2.11, 2.16 (12H, s, Me); 3.44−3.50 (2H, m, $OCH_2\underline{CH_2}N_3$); 3.64−3.71 (1H, m, $O\underline{CH_2}CH_2N_3$); 3.84−3.91 (1H, m, $O\underline{CH_2}CH_2N_3$); 4.02−4.08 (1H, m, H5); 4.11−4.15 (1H, dd, $J = 2.2$, 12.2 Hz, H6); 4.26−4.32 (1H, dd, $J = 5.3$, 12.2 Hz, H6); 4.87 (1H, d, $J = 1.3$ Hz, H1); 5.26−5.39 (3H, m, H2, 3, 4). ^{13}C NMR: (75.5 mHz, $CDCl_3$, δ): 20.77, 20.83, 20.86, 20.99 (4C, CH_3); 50.48 (1C, CH_2N_3); 62.58 (1C, CH_2); 66.12 (1C, CH); 67.17 (1C, CH_2O); 68.98 (2C, CH); 69.5 (1C, CH); 97.87 (1C, CH); 169.88, 169.91, 170.12, 170.72 (4C, C═O). LR-MS (ESI): Calcd for $C_{16}H_{23}N_3O_{10}Na$ $[M+Na]^+$, 440.36; found, 440.2.

*c. Synthesis of 2′-Aminoethyl-2,3,4,6-tetra-O-acetyl-α-D-mannopyranoside (***5***).* A suspension of compound **2** (0.8 g) and activated palladium on charcoal 10% Pd/C (120 mg) in anhydrous MeOH (32 mL) was stirred under H_2. After 30 min, the reaction was stopped and the mixture was filtered. The filtrate was concentrated in vacuum to give the title compound **5** in 46.5% yield as a fluffy white solid. ^{1}H NMR: (300 mHz, $CDCl_3$, δ): 2.0, 2.04, 2.10, 2.16 (12H, s, Me); 2.90−2.93 (2H, t, $OCH_2\underline{CH_2}NH_2$); 3.46−3.53 (1H, m, $O\underline{CH_2}CH_2NH_2$); 3.71−3.78 (1H, m, $O\underline{CH_2}CH_2NH_2$); 3.99−4.04 (1H, m, H5); 4.08−4.13 (1H, dd, $J = 2.1$, 12.2 Hz, H6); 4.26−4.32 (1H, dd, $J = 5.3$, 12.2 Hz, H6); 4.85 (1H, d, $J = 1.5$ Hz, H1); 5.25−5.38 (3H, m, H2, 3, 4). ^{13}C NMR: (75.5 mHz, $CDCl_3$, δ): 20.82, 20.87, 21.01 (4C, $4CH_3$); 41.48 (1C, CH_2NH_2); 62.63 (1C, CH_2); 66.29 (1C, CH); 68.66 (1C, CH_2O); 69.20, 69.62, 70.66 (3C, CH); 97.91 (1C, CH); 169.85, 170.11, 170.21, 170.80 (4C, C═O). LR-MS (ESI): Calcd for $C_{16}H_{24}N_3O_{10}$ $[M+H]^+$, 392.37; found, 392.3.

*d. Synthesis of 2′-Acrylamidoethyl-2,3,4,6-tetra-O-acetyl-α-D-mannopyranoside (***8***).* A solution of compound **5** (3 g) in anhydrous methylene chloride (80 mL) cooled in an ice bath, TEA (1.28 mL), and acryloyl chloride (0.69 mL) were added dropwise under an argon atmosphere. The reaction mixture was allowed to come to room temperature slowly and was stirred overnight. The solution was then washed with water and 1 N HCl and then sodium bicarbonate solution and water. The organic phase was dried over anhydrous sodium sulfate and concentrated in vacuum to yellow syrup (2.3 g). Flash column chromatography on silica in EtOAc/hexanes (10:1, Rf 0.45) gave pure compound as colorless syrup (1.1 g, yield 32.2%). ^{1}H NMR: (300 mHz, $CDCl_3$, δ): 2.01, 2.05, 2.10, 2.16 (12H, s, Me); 3.54−3.67 (3H, m, $OCH_2\underline{CH_2}NH-$, $O\underline{CH_2}CH_2NH-$); 3.80−3.85 (1H, m, $O\underline{CH_2}CH_2NH-$); 3.95−4.00 (1H, m, H5); 4.09−4.14 (1H, dd, $J = 2.3$, 12.2 Hz, H6); 4.22−4.28 (1H, dd, $J = 5.7$, 12.2 Hz, H6); 4.83 (1H, dd, $J = 1.5$ Hz, H1); 5.22−5.36 (3H, m, H2, 3, 4); 5.66−5.70 (1H, dd, $J = 1.33$, 10.1 Hz, $-CH=\underline{CH_2}$); 6.06−6.20 (2H, m, NH, $-\underline{CH}=CH_2$); 6.29−6.35 (1H, dd, $J = 1.5$, 16.9 Hz, $-CH=\underline{CH_2}$). ^{13}C NMR: (75.5 mHz, $CDCl_3$, δ): 20.86, 20.88, 21.03 (4C, $4CH_3$); 39.29 (1C, CH_2NH); 62.67 (1C, CH_2); 66.32 (1C, CH); 67.72 (1C, CH_2O); 68.93, 69.15, 69.52 (3C, CH); 97.94 (1C, CH); 127.10 (1C, CH_2═CH); 130.73 (1C, CH═CH_2); 165.78 (1C, CONH); 169.85, 170.25, 170.82 (4C, C═O). LR-MS (ESI): Calcd for $C_{19}H_{27}NO_{11}Na$ $[M+Na]^+$, 468.41; found, 468.2.

*e. Synthesis of 2′-Acrylamidoethyl-α-D-mannopyranoside (***11***).* To a solution of compound **8** (1 g, 23 mmol) in anhydrous methanol (20 mL) was added 25% sodium methoxide in methanol (468 μL, 23 mmol) dropwise. The reaction mixture was stirred for 90 min at room temperature. Dowex cation-exchange resin (H form) was added to adjust the pH between 6 and 7 and filtered. The filtrate was concentrated in a rotary evaporator. The residue was dissolved in water and filtered again. After freeze-drying, the title compound **11** was obtained in 83% yield as a white solid. ^{1}H NMR: (300 mHz, D_2O, δ): 3.45−3.65 (5H, m, $OCH_2\underline{CH_2}NH-$, $O\underline{CH_2}CH_2NH-$, H5); 3.72−3.91 (5H, m, H2,3,4,6); 4.83−4.84 (1H, d, $J = 1.5$ Hz, H1); 5.72−5.76 (1H, dd, $J = 1.9$, 9.7 Hz, $-\underline{CH}=CH_2$); 6.13−6.19 (1H, dd, $J = 1.9$, 17.1 Hz, $-CH=\underline{CH_2}$); 6.21−6.30 (1H, dd, $J = 9.7$, 17.2 Hz, $-CH=\underline{CH_2}$). ^{13}C NMR: (75.5 mHz, D_2O, δ): 39.10 (1C, CH_2NH); 60.91 (1C, CH_2); 65.87 (1C, CH); 66.71 (1C, CH_2O); 70.10, 70.20, 72.88 (3C, CH); 99.79 (1C, CH); 127.56 (1C, CH_2═CH); 129.95 (1C, CH═CH_2); 168.83 (1C, CONH). LR-MS (ESI): Calcd for $C_{11}H_{19}NO_7Na$ $[M+Na]^+$, 300.26; found, 300.2.

Details of the synthesis and characterization of glucose and galactose monomers 2′-acrylamidoethyl-β-D-glucopyranoside (**12**) and 2′-acrylamidoethyl-β-D-galactopyranoside (**13**) are given in the Supporting Information.

Synthesis of Amide Derivatives of Surface Initiator (11-(2′-Chloro-propionamido)-undecyl-trichlorosilane (14). A solution of 1-amino-10-undecene (2 g) in anhydrous THF (20 mL) cooled in an ice bath, pyridine (1.2 mL), and 2-chloropropionyl chloride (1.3 mL) were then added dropwise via syringe under an argon atmosphere. The reaction mixture was allowed to come to room temperature slowly and was stirred overnight. The reaction solution was diluted by hexane and washed with 2 N HCl and deionized water. The organic phase was dried over anhydrous sodium sulfate and concentrated in vacuum to light-yellow oil. Flash column chromatography on silica in EtOAc/hexanes (1:4) gave the pure product (compound **13**) as a colorless oil (2.3 g, yield 75%). ^{1}H NMR: (300 MHz, $CDCl_3$, δ): 1.28−1.60 (14H, m, 7 × CH_2); 1.73−1.75 (3H, d, CH_3); 2.0−2.04 (2H, q, $-CH_2-CH=CH_2$); 3.23−3.30 (2H, q, $-N-CH_2-$); 4.37−4.44 (H, q, −CH−); 4.91−5.02 (2H, $-CH=CH_2$); 5.74−5.88 (1H, m, $-CH=CH_2$); 6.56 (1H, s, −NH−).

Scheme 1. Chemical Structures of 2′-Acrylamidoethyl-α-D-mannopyranoside (Compound **11**), 2′-Acrylamidoethyl-β-D-glucopyranoside (Compound **12**), and 2′-Acrylamidoethyl-β-D-galactopyranoside (Compound **13**)

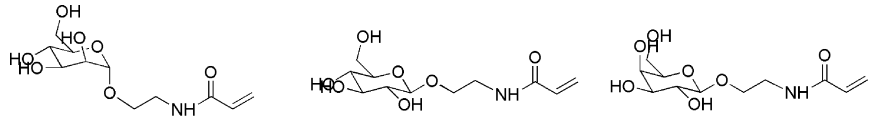

11 **12** **13**

To a 50 mL flask, 1 g of compound **13** and 5.3 g of trichlorosilane were added, followed by the addition of 8 μL of Karstedt catalyst via micropipette. The mixture was allowed to stir at room temperature for 5 h. The excess trichlorosilane was removed under reduced pressure. The residue was diluted with 0.5 mL of anhydrous toluene. The solution was quickly filtered through a plug of silica gel to remove the catalyst. The filtrate was concentrated in vacuum to give the title compound **14** as light-yellow oil. ^{1}H NMR: (300 MHz, $CDCl_3$, δ): 1.28−1.61 (18H, m, 9 × CH_2); 1.72−1.75 (3H, d, CH_3); 3.24−3.31 (2H, q, −N−CH_2−); 4.38−4.45 (1H, q, −CH−); 6.56 (1H, s, −NH−).

Synthesis of Poly(2′-acrylamidoethyl-2,3,4,6-tetra-*O*-acetyl-α-D-mannopyranoside) (PAAETAM) Brushes from Hydroxyl Protected Monomer. Copper(II) chloride ($CuCl_2$, 3 mg, 0.02 mmol), copper(I) chloride (CuCl, 7 mg, 0.07 mmol), and Me_6TREN (52 μL, 0.18 mmol) were added successively to a glass tube, followed by the addition of 12 mL of DMSO. The solution was degassed with three freeze−pump−thaw cycles. The solution was then transferred to the glovebox. The catalyst solution (0.73 mL) was drawn and added to the vial, which contained 2′-acrylamidoethyl-2,3,4,6-tetra-*O*-acetyl-α-D-mannopyranoside (0.65 g, 1.46 mmol). After the monomer was completely dissolved, the surface initiator (11-(2′-chloro-propionamido)-undecyl-trichlorosilane) deposited silicon wafer was immersed in the polymerization mixture. Soluble-free initiator, 22 μL of methyl 2-chloropropionate in DMSO (stock solution 440 μL in 4 mL of DMSO), was added immediately to the reaction mixture. The polymerization was allowed to proceed at RT (22 °C) for 24 h. The substrate was then thoroughly rinsed with methanol and sonicated in methanol for 30 min. The soluble polymer formed along with the surface-grafted polymer was collected by passing through a column packed with basic alumina and the polymer was precipitated from diethyl ether.

Deprotection of PAAETAM. To a solution of PAAETAM (24 mg) in anhydrous methanol (10 mL) was added 25% sodium methoxide in methanol (11 μL, 23 mmol) dropwise. The reaction mixture was stirred for 5 h at room temperature. Dowex cation-exchange resin (H form) was added to adjust the pH to 6 to 7 and filtered. The filtrate was concentrated in vacuum.

Deprotection of the Surface-Grafted PAAETAM. To a vial containing PAAETAM grafted substrate, anhydrous methanol (5 mL) and 25% sodium methoxide in methanol (5 μL) were added subsequently. The samples were removed from the vial after 20 h and thoroughly washed with methanol and deionized water.

Synthesis of Poly(2′-acrylamidoethyl-α-D-mannopyranoside) (PAAEM) Brushes from Hydroxyl Free Monomer. Copper(II) chloride ($CuCl_2$, 1.35 mg, 0.01 mmol), copper(I) chloride (CuCl, 8 mg, 0.08 mmol), and Me_6TREN (52 μL, 0.18 mmol) were added successively to a glass tube, followed by the addition of Milli Q water (12 mL). The solution was degassed with three freeze−pump−thaw cycles. The solution was then transferred to the glovebox. The solution (1 mL) was drawn and added to the vial, which contained 2′-acrylamidoethyl-α-D-mannopyranoside (50 mg). After the monomer was completely dissolved, surface-initiator-modified substrate (ester derivative) was immersed in the solution. Soluble methyl 2-chloropropionate in water with defined concentration was then added to the reaction solution. The surface-initiated polymerization was allowed to proceed at RT (22 °C) for 24 h. The substrates were then thoroughly rinsed with water and sonicated in water for 30 min, followed by drying with nitrogen gas. The solution was dialyzed against deionized water and then freeze-dried.

PAAEGlc brushes and PAAEGal brushes were synthesized using a similar procedure. All brush structures were characterized in terms of thickness, graft density, molecular weight, contact angle measurements, and AFM measurements.

Synthesis of Other Glucose-Containing Brushes. PGAMA and PMAGlc brushes and brushes were synthesized following the polymerization procedures reported in the literature.[28,35] and were characterized using ellipsometry and contact angle measurements.

Nonspecific Protein Adsorption Studies. Initially, the substrates were equilibrated with phosphate-buffered saline (PBS) for 15 min; then, the protein solutions were introduced. The protein solutions were centrifuged at 10 000 rpm (9300 rcf) for 5 min. Supernatant was used in the protein adsorption study. The final concentrations of BSA and Fb were 1 and 0.25 mg/mL, respectively.

After incubation for 1 h at room temperature, the samples were removed and washed with PBS buffer three times to remove loosely adsorbed proteins. The images of the protein-adsorbed surfaces were taken by a fluorescence microscope (NikonEclipse TE 2000-U with an X-Cite 120 fluorescence illumination system, FITC and rhodamine filters, and a DS-U1 suit digital camera). The fluorescence images were transferred to gray scale by Adobe Photoshop 6.0, and intensity was taken to be linearly related to the quantity of adsorbed proteins on the surface.[42,43] The initiator-modified substrate was chosen as the control sample. The fluorescence intensity of the control sample was set as 100%, and the adsorption of proteins on various polymer grafted surfaces was normalized on the basis of the calibration scale. After the fluorescence measurement, the substrates were washed with water three times. The dry thickness of the brushes after protein adsorption was then determined by ellipsometry.

Specific Protein Interaction Studies. The studies followed the same procedures described above except for the use of Con A and PBS buffer containing 1 mM $CaCl_2$ and 0.1 mM $MnCl_2$. The pH of the buffer was adjusted to 4.8. Con A is a lectin that specifically binds mannose and glucose residues.[25,26] The final concentration of Con A solution was 0.2 mg/mL.

Results and Discussion

Synthesis of N-Substituted Acrylamide Derivatives of Unprotected Glycomonomers. Chemical structures of synthesized glycomonomers containing mannose, galactose, and glucose residues are shown in Scheme 1. The synthesis of 2′-acrylamidoethyl-α-D-mannopyranoside is outlined in Scheme 2. 1,2,3,4,6-Penta-*O*-acetyl-D-mannose was readily obtained by peracetylation of D-mannose by using excess of acetic anhydride in pyridine serving both as solvent and catalyst. Obtained peracetylated mannose was a mixture of α- and β-anomer in a 4:1 ratio (from ^{1}H NMR analysis). Glycosylation of mannose pentaacetate with 2-azidoethanol, which was easily accessible from 2-bromoethanol and sodium azide, in the presence of $BF_3 \cdot Et_2O$ gave α glycosides as a sole product. The azide group was then reduced to amine group via the Pd/C-catalyzed hydrogenation. We found that a portion of the resulting primary amine was self-condensed to generate symmetric secondary amine (bis(2,3,4,6-tetra-*O*-acetyl-α-D-mannopyranosyloxyethyl)amine) when the reaction time was extended beyond 30 min. When the reaction time was changed from 30 min to 2 h, a

Scheme 2. Synthesis of 2′-Acrylamidoethyl-α-D-mannopyranoside

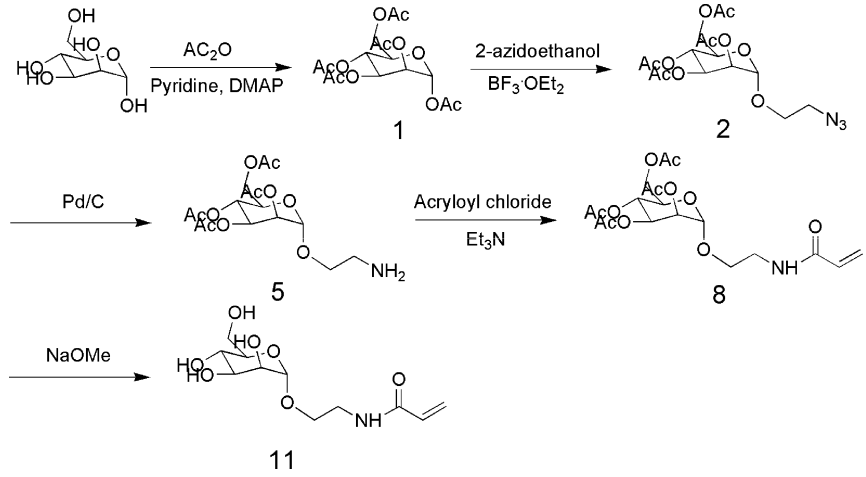

new MS peak at 766.4 Da, which corresponds to the positively charged symmetric secondary amine, appeared in the spectrum of resulting product (Supporting Information, Figure S1). This observation is consistent with the reports that primary amine can undergo self-condensation and transform to a secondary amine in the presence of palladium catalyst.[44,45] By controlling the reaction time, we can achieve the conversion of azide to primary amine without the formation of side product, however, the yield is sacrificed (Figure S2, Supporting Information). The 2′-aminoethyl-2,3,4,6-tetra-*O*-acetyl-α-D-mannopyranoside (compound **5**) was then treated with acryloyl chloride in the presence of triethylamine to give 2′-acrylamidoethyl-2,3,4,6-tetra-*O*-acetyl-α-D-mannopyranoside. It is important that the formation of secondary amine should be prevented before this step. *N*,*N*-Di(2,3,4,6-tetra-*O*-acetyl-α-D-mannopyranosyloxyethyl)acrylamide (formed by the reaction between secondary amine and acryloyl chloride) and main product (compound **8**) have similar polarity values, and it was difficult to purify this mixture by column chromatography. The deacetylation of the 2′-acrylamidoethyl-2,3,4,6-tetra-*O*-acetyl-α-D-mannopyranoside (compound **8**) gave the final product (compound **11**). Purity of the final monomer has great influence on the polymerization. (See the next section.) A similar route was followed for the synthesis of 2′-acrylamidoethyl-β-D-glucopyranoside (**12**) and 2′-acrylamidoethyl-β-D-galactopyranoside (**13**).

Surface Initiator Functionalization. Besides the ester-functionalized SI-ATRP initiator (11-(2-bromo-2-methyl)-propionyloxy)-undecyltrichlorosilane), a new amide derivative of initiator was also synthesized. The ellipsometry measurements gave thicknesses of 2.8 ± 0.4 and 2 ± 0.1 nm, respectively, for the amide- and ester-functionalized initiator layers. The water contact angle on amide-based initiator (62.9 ± 0.2°) layer was smaller than that on an ester-based initiator (74.5 ± 1.1°) layer because the amide group is relatively more hydrophilic than the ester group. XPS data collected from the two initiator-modified Si wafers were presented in Figure S4 of the Supporting Information. The Cl (2p) and N (1s) appearing at 200.6 and 400.3 eV, respectively, confirmed the formation of amide-based initiator layer on Si wafer. The Br (3d) signal situated at 69.7 eV, confirmed the presence of ester-based initiator layer on Si wafer.

Synthesis of Glycopolymer Brushes. We adopted two routes for the synthesis of glycopolymer layer containing mannose units by (i) polymerization of acetate-protected monomer, followed by the deprotection of acetate groups in the surface grafted polymer (Scheme 3A) and (ii) polymerization of unprotected monomer directly from the surface (Scheme 3B). The study was designed to help us understand the polymerization properties of both types of monomers and achieve the goal of producing fully functional glycopolymer layer containing carbohydrate residues.

We estimated the grafting density (σ) for glycopolymer brushes by using the equation $\sigma = (h\rho N_A)/M_n$, where M_n is the molecular weight of free polymer in the solution, N_A is Avogadro's number, h is the polymer layer "dry" thickness measured by elliposometer, and ρ is the density of glycopolymer. (We assumed that the density of glycopolymer brushes is equal to 1 g/cm^3.) Assuming that the molecular weight of the glycopolymer grown in solution is similar that of surface-grafted glycopolymer,[28,46] the grafting density of tethered glycopolymer chains was estimated. Although this is not a very accurate method for calculation of graft density of the surface-grafted polymer layers, it is a regular practice, especially for polymer chains grown on flat surfaces, and is widely accepted in the literature.[28,46]

i. SI-ATRP of PAAEM Brushes via Protected Monomer Route. Initially, we explored the preparation of glycopolymer brushes by using 2′-acrylamidoethyl-2,3,4,6-tetra-*O*-acetyl-α-D-mannopyranoside, followed by the deprotection of acetate groups. The concentration of sodium methoxide was critical in the deprotection of acetate group in the grafted glycopolymer layer. The amide-functionalized initiator layer was tested initially under the deprotection conditions to ensure its stability. At relatively high concentration (e.g., 0.5 wt % NaOMe in MeOH), the amide-functionalized initiator layer was destroyed, as evident from the decrease in thickness from 2.8 to 1.2 nm. Therefore, a lower concentration of sodium methoxide was chosen for the study (0.025 wt % NaOMe in MeOH). In the case of acetate-protected glycopolymer brushes, upon treatment with NaOMe, the thickness of the grafted layer decreased from 7.8 ± 0.4 to 5.5 ± 0.3 nm in 22 h. The water contact angle decreased from 53.8 ± 1.3 to 33.5 ± 0.8° (Table S1 of the Supporting Information). The thickness and contact angle did not show noticeable change by extending the hydrolysis time to several days. In comparison with the water contact angles of the glycopolymer brushes prepared directly from the deprotected monomer (7.2 ± 1.3°) (see the next section), we confirmed that the deprotection of acetate group in the grafted glycopolymer layer was not complete. The incomplete deprotection may be brought by limited access of reactant to highly dense glycopolymer grafted surface. In contrast, the acetate group of free polymer generated in solution can be effectively removed by

Scheme 3. Synthesis of Poly(2′-acrylamidoethyl-α-D-mannopyranoside) Brushes by Polymerizing Protected Monomer (2′-Acrylamido-2,3,4,6-tetra-*O*-acetyl-α-D-mannopyranoside), Followed by Deprotection Procedure (A) or by Polymerizing Deprotected Monomer (2′-Acrylamidoethyl-α-D-mannopyranoside) Directly (B). The Brushes Prepared by Different Routes have Difference in the Structure of Surface Initiator

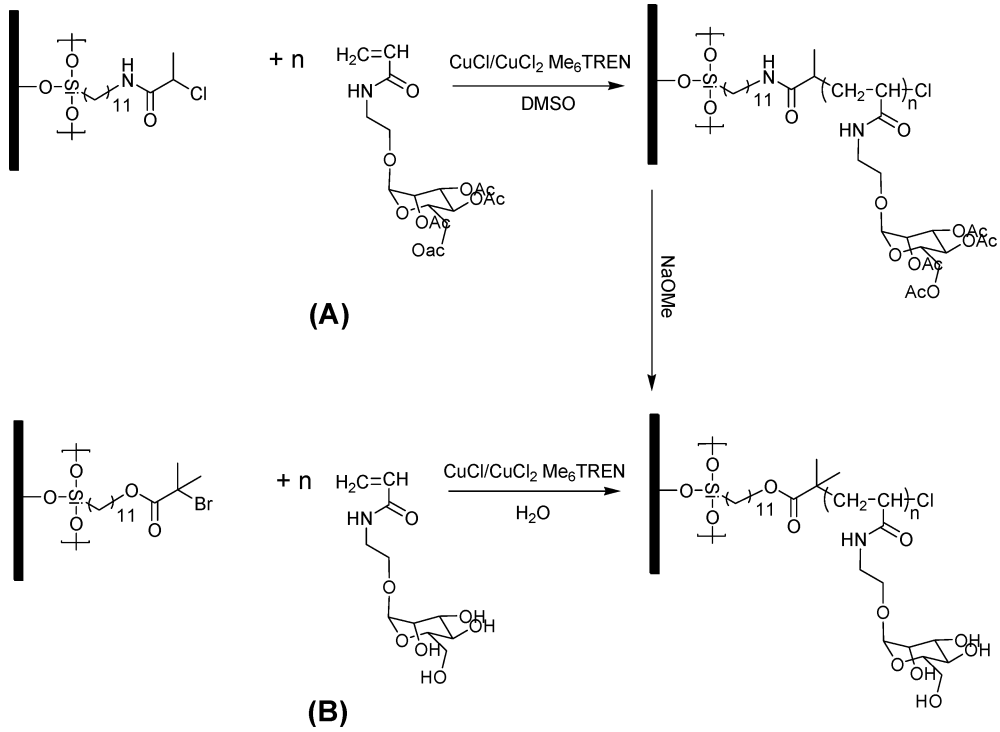

Table 1. Effect of Halogen, Ligand and Solvents on the Polymerization of 2′-Acrylamidoethyl-α-D-mannopyranoside[a]

polymer	ligand	solvent	$[CuCl_2]/[CuCl]$	M_n	PDI	dry thickness (nm)	grafting density (chains/nm^2)	static water contact angle (°)
1		H_2O	0	250 000	2.1	25.2 ± 0.2	0.06	5.3 ± 1.5
2		H_2O	1/16	66 000	1.7	17.9 ± 0.8	0.16	6.2 ± 1.7
3		H_2O	1/8	83 000	1.4	24.1 ± 0.3	0.17	4.4 ± 0.9
4	Me_6TREN	H_2O	1/4	51 000	1.5	11.7 ± 0.4	0.14	5.4 ± 1.3
5		H_2O/DMF 1:1	1.8	38 000	1.4	6.6 ± 0.3	0.10	5.6 ± 0.7
6		H_2O/DMSO 1:1	1/8	60 000	3.6	7.9 ± 0.5	0.08	4.8 ± 1.7
7		H_2O	$CuBr_2/CuBr$:1/8	58 000[b]	4.5	14.3 ± 0.2	0.15	4.1 ± 1.3
8	HMTETA	H_2O	1/8	55 000	3.2	5.4 ± 0.1	0.06	5.4 ± 1.9

[a] Polymerization conditions: M: 2′-acrylamidoethyl-α-D-mannopyranoside, 5% W/V. Initiator: methyl 2-chloropropionate, [I] = 1.25 mM, reaction time: 24 h, RT. [b] Polymerization conditions: [M] = 5% W/V. Initiator: methyl 2-bromoisobutyrate, [I] = 1.25 mM, reaction time: 24 h, RT (22 °C).

using sodium methoxide in methanol. Figure S5 of the Supporting Information shows the ^{1}H NMR spectra of polymer before (I) and after deprotection (II). The disappearance of four sharp peaks around 2 ppm, which were assigned to the acetate groups, confirmed the completion of deprotection. The number-average molecular weight of polymer after deprotection was 14 000, whereas the PDI value was 4.5. The broad polydispersity indicated that the polymerization control was very poor.

ii. SI-ATRP of PAAEM Brushes via Unprotected Monomer Route. Because of the inefficient removal of acetate groups in the grafted glycopolymer layer and other complications, we prepared the mannose-containing polymer graft layers using unprotected 2′-acrylamidoethyl-α-D-mannopyranoside by SI-ATRP. Silicon wafer modified with ester-based ATRP initiator was used as a substrate for this study. Several experimental conditions were investigated to improve the control of polymerization in solution and from surface.

Effect of Halogen. The polymerization behaviors of the bromine-containing system (alkyl bromide as the initiator, CuBr/$CuBr_2$/Me_6TREN as the catalyst) and the chlorine-containing system (alkyl chloride, CuCl/$CuCl_2$/Me_6TREN) were studied and compared. The chlorine system gave a narrower distribution of glycopolymer chains than the bromine system (polymer 7 in Table 1). This is consistent with the report on polymerization of acrylamide derivatives by using bromine system because Br chain ends are more susceptible to nucleophilic substitution or elimination reactions in protic solvents.[47,48] The loss of terminal C−Br groups will effectively "kill" the polymer chain ends, and a relatively broad molecular weight distribution can be expected. The use of chloride initiator in conjunction with CuCl/$CuCl_2$/Me_6TREN resulted in better control of the polymerization because chlorine chain ends are better preserved during the polymerization process because of the decrease in nucleophilic displacement.[49] The effect of halogen in surface initiator on polymerization was also investigated. The ester-based surface initiator gave better surface-initiated polymerization, as noted from the thickness of the grafted layer. Under similar polymerization conditions, glycopolymer brushes grown from ester initiator gave a thickness of 17.9 ± 0.8 nm (Table 1, entry 2) in comparison with 14.2 ± 1.3 nm thickness produced by amide-based surface initiator (having a secondary chlorine).

The effect of molar ratio of Cu(I)/Cu(II) on polymerization was also investigated in detail. Without the addition of deactivator, $CuCl_2$, the polydispersity of resulting glycopolymer (poly-

mer 1) was broad (PDI = 2.1). The use of a mixture of CuCl/Me_6TREN and $CuCl_2$/Me_6TREN complex (molar ratio 8:1) resulted in a decrease in polydispersity to 1.4 (polymer 3). The addition of more $CuCl_2$ (molar ratio of Cu(I)/Cu(II) 4:1) complex did not show any large change in polydispersity. The thickness of brushes also showed dependence on the molar ratio of Cu(I)/Cu(II). At a molar ratio of 8:1, the highest thickness of the grafted layer was achieved while the polydispersity of free polymer was maintained as low as 1.4.

Effect of Ligands. 1,1,4,7,10,10-Hexamethyltriethylenetetramine (HMTETA), which is considered to be a good ligand for the acrylamide polymerizations,[50,51] was used for the polymerization of mannose-containing monomer. The polydispersity of resulting PAAEM (polymer 8 in Table 1) was high (>3.2), indicating a poor control of the polymerization. The thickness for the PAAEM brushes was also low (5.4 nm) with a grafting density 0.06 chains/nm^2. When Me_6TREN was employed as a ligand, substantial improvement in polymerization was observed, unlike other commonly used ATRP ligands.[52,53] The resulting glycopolymers showed lower polydispersity (PDI 1.4 to 1.7).

Effect of Solvents. Polymerization was carried out in different solvent systems, and the results are shown in Table 1. The thickness of PAAEM brushes prepared in the mixed solvent DMF/H_2O was much lower than those prepared in H_2O. Polymerization in mixed solvent DMF/H_2O produced low molecular weight with similar polydispersity (PDI = 1.4), whereas H_2O/DMSO gave broader dispersity of chains (PDI = 3.6).

Effect of Addition of Soluble ATRP Initiator. The thickness of PAAEM can be controlled by the addition of free soluble initiator in the polymerization medium. By increasing the concentration of free initiator from 0.55 to 3.75 mM, the thickness of grafted polymer layer proportionally decreased from 34.7 to 10.3 nm, whereas the calculated grafting density of brushes maintained relatively constant at 0.17 chains/nm^2. There was also proportional decrease in the thickness of the brush with decrease in molecular weight of free polymer (Figure 1).

When unpurified monomer mixture (previously described) containing 7% *N*,*N*-di(α-D-mannopyranosyloxyethyl)acrylamide (Figure S3 of the Supporting Information) was used for polymerization, both thickness and grafting density were decreased. For instance, under similar conditions, the purified AAEM monomer gave a layer thickness of 34.7 nm with a graft density (0.17 chains/nm^2), whereas the mixture of monomers (93 mol % AAEM and 7 mol % *N*,*N*-di(α-D-mannopyranosyloxyethyl)acrylamide) gave a polymer layer thickness and grafting density 19.6 nm and 0.09 chains/nm^2, respectively. This large difference showed the importance of the previously mentioned purification step.

Effect of Different Carbohydrates in the Monomer. We prepared PAAEGlc brushes and PAAEGal brushes from their respective unprotected monomer (Scheme 1) by adopting a similar polymerization condition as that used in the polymerization kinetics study (see the caption of Figure 3), and the polymerization time was kept constant at 24 h. The results are summarized in Table 2. The thickness for the PAAEGlc and PAAEGal brushes was slightly higher than that for PAAEM brushes, whereas the grafting densities were 0.12 chains/nm^2, respectively.

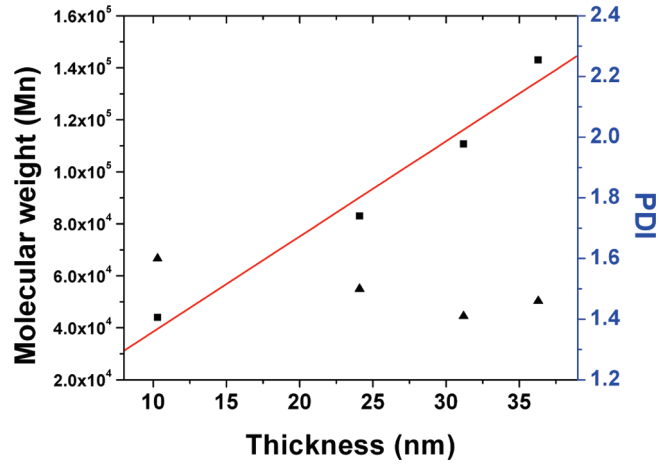

Figure 1. Relationship between grafted PAAEM layer thickness and molecular weight of free polymer (■). Polydispersity of free polymer (▲) formed along with surface initiated polymer. Polymerization condition: [M] = 5% W/V. Initiator: methyl 2-chloropropionate, [CuCl]/[$CuCl_2$]/[Me_6TREN] = 8/1/18 mM, RT. Ester-based surface initiator was used.

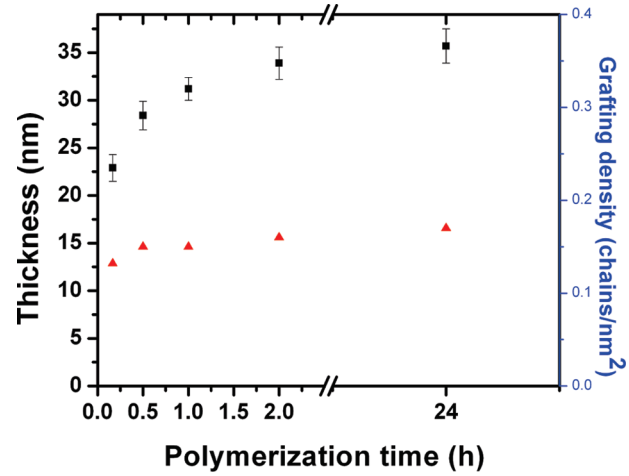

Figure 2. Thicknesses (■) and grafting densities (▲) of PAAEM brushes with polymerization time. Polymerization condition: [M] = 5% W/V, Initiator: methyl 2 chloropropionate, [I] = 0.75 mM, [CuCl]/[$CuCl_2$]/[Me_6TREN] = 8/1/18 mM, RT, ester-based surface initiator was used.

Kinetics of Polymerization of 2′-Acrylamidoethyl-α-D-mannopyranoside. We monitored the growth of PAAEM brushes during SI-ATRP by measuring grafted polymer layer thickness. Figure 2 shows the increase in polymer layer thickness measured by ellipsometry as a function of polymerization time. In the first 10 min, thickness increased rapidly to 22.9 ± 1.4 nm, indicating a very fast initial polymerization. After the reaction time was extended to 2 h, thickness increased to 33.9 ± 1.7 nm. Further extending the reaction time to 24 h resulted in only a small change in the thickness. Two possible reasons may be accounted for the arrest of the growth of brushes: catalyst deactivation and chain termination by bimolecular coupling or

Table 2. Characteristics Results for Poly(2′-acrylamidoethyl-β-D-galactopyranoside) and Poly(2′-acrylamidoethyl-β-D-glucopyranoside) Brushes and Corresponding Free Polymer in Solution

polymer	M_n	PDI	brush dry thickness (nm)	graft density (chains/nm^2)	water contact angle (°)
poly(2′-acrylamidoethyl-β-D-galactopyranoside)	220 000	1.4	42.7 ± 0.82	0.12	6.9 ± 1.2
poly(2′-acrylamidoethyl-β-D-glucopyranoside)	209 000	1.5	42.8 ± 0.61	0.12	5.6 ± 0.7

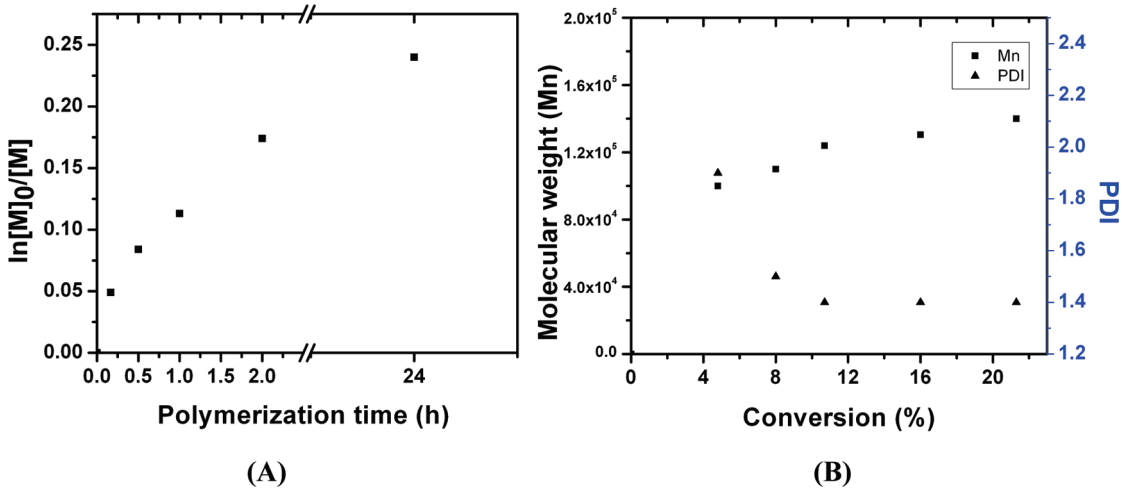

Figure 3. (A) First-order kinetic plot for surface-initiated ATRP of 2′-acrylamidoethyl-α-D-mannopyranoside in H_2O. (B) Dependence of molecular weight (M_n) and molecular weight distribution (M_w/M_n) on monomer conversion. Polymerization condition: [M] = 5% W/V. Initiator: methyl 2-chloropropionate, [I] = 0.75 mM, [CuCl]/[$CuCl_2$]/[Me_6TREN] = 8/1/18 mM, RT. Ester-based surface initiator was used.

Table 3. Characteristics Results of Brushes Containing Glucose with Different Structures and Corresponding Free Polymer in Solution

glucose-containing brushes	dry thickness (nm)	grafting density (chains/nm^2)	M_n	PDI	water contact angle (°)
PAAEGlc	42.8 ± 0.6	0.12	209 000	1.5	5.6 ± 0.7
PGAMA	37.2 ± 0.2	0.3	73 600	1.6	19.8 ± 1
PMAGlc	29.9 ± 0.1	0.25	72 000	1.2	39.8 ± 1.3

disproportionation. To examine whether the catalyst was deactivating during the reaction, we carried out a control experiment in which fresh catalyst[54,55] was added after 24 h of polymerization. This fresh catalyst addition did not lead to any significant change in polymer growth, indicating that catalyst deactivation was not the primary reason for cessation of layer growth. Therefore, we attribute the chain arrest to either bimolecular coupling or disproportionation.

The molecular weights of free polymer in solution and total conversion were also monitored during the polymerization. Figure 3 shows the first-order kinetic plot (A) and the evolution of M_n with conversion for ATRP of AAEM in water (B). The initial rate of the polymerization was very fast (the M_n rapidly increased to 100 000), whereas the total monomer conversion (contributions from both solution polymerization and surface polymerization) reached 4.8% in 10 min. After the reaction time was extended to 2 h, the M_n increased to 135 000, whereas the total conversion increased to 16%. After 24 h, the M_n increased to 140 000 with the monomer conversion to 22.3%. The polydispersity of the chains decreased with monomer conversion and remained relatively constant above 10.7% conversion. Although the unusual nonlinear nature of the first-order kinetic plot and the evolution of M_n with conversion are indicative of termination reactions in the early stage, the symmetrical unimodal feature of GPC traces of the glycopolymer at high conversions with relatively narrow molecular weight distribution is telling a different story (Figure S7, Supporting Information). Similar unusual polymerization behavior has been observed by our group[56,57] as well as other investigators on surface initiated polymerizations in aqueous solutions.[58−62] Messersmith observed similar rapid initial growing rate during the SI-ATRP of methyl methacrylate macromonomers with oligo(ethylene glycol) side chains.[58] Xu also reported that there was a rapid increase in the degree of polymerization of GAMA during the initial stage of polymerization.[32] The high dielectric constant, especially water, increased the activity of the catalyst.[63,64] The high activity of Cu(I) complex brings a high concentration of active species (or radicals) and, subsequently, a high polymerization rate in the initial stage. In aqueous ATRP, water acts as both an accelerator to increase the activity of the catalyst and a diluent.

Surface Characterization. The PAAEM grafted layers with thicknesses ranging from 10 to 40 nm gave highly hydrophilic surface layers, as evident from the very low water contact angles (<10°) (Table 1). PAAEGlc and PAAEGla brushes also behaved similarly (Table 2). The water contact angles of newly synthesized brushes are much lower than the reported glycopolymer brushes having similar thickness. A comparison of glycopolymer brushes containing glucose units is given in Table 3. The pronounced hydrophilic character of PAAEGlc grafted surface maybe attributed to the unprotected carbohydrate unit within the grafted layer. Figure 4 shows the ATR-FITR spectra of PAAEM, PAAEGal, and PAAEGlc brushes. The characteristic peaks at 1647 and 1550 cm^{-1} correspond to the C═O stretching vibration and the N−H bending vibrations of the amide group.

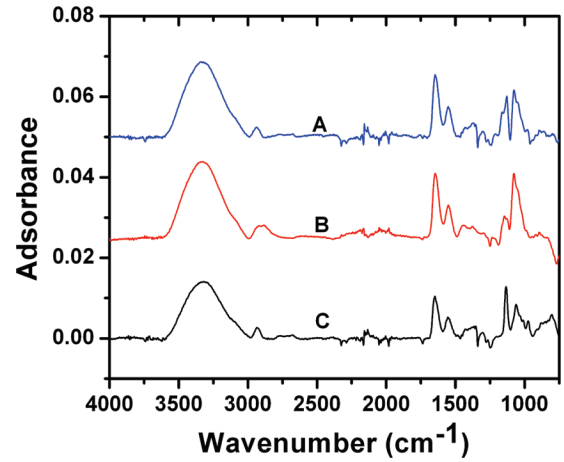

Figure 4. FTIR spectra of glycopolymer brushes containing different carbohydrate units: (A) PAAEGlc brush (38.4 nm), (B) PAAEGal brush (36.8 nm), and (C) PAAEM brush (27 nm).

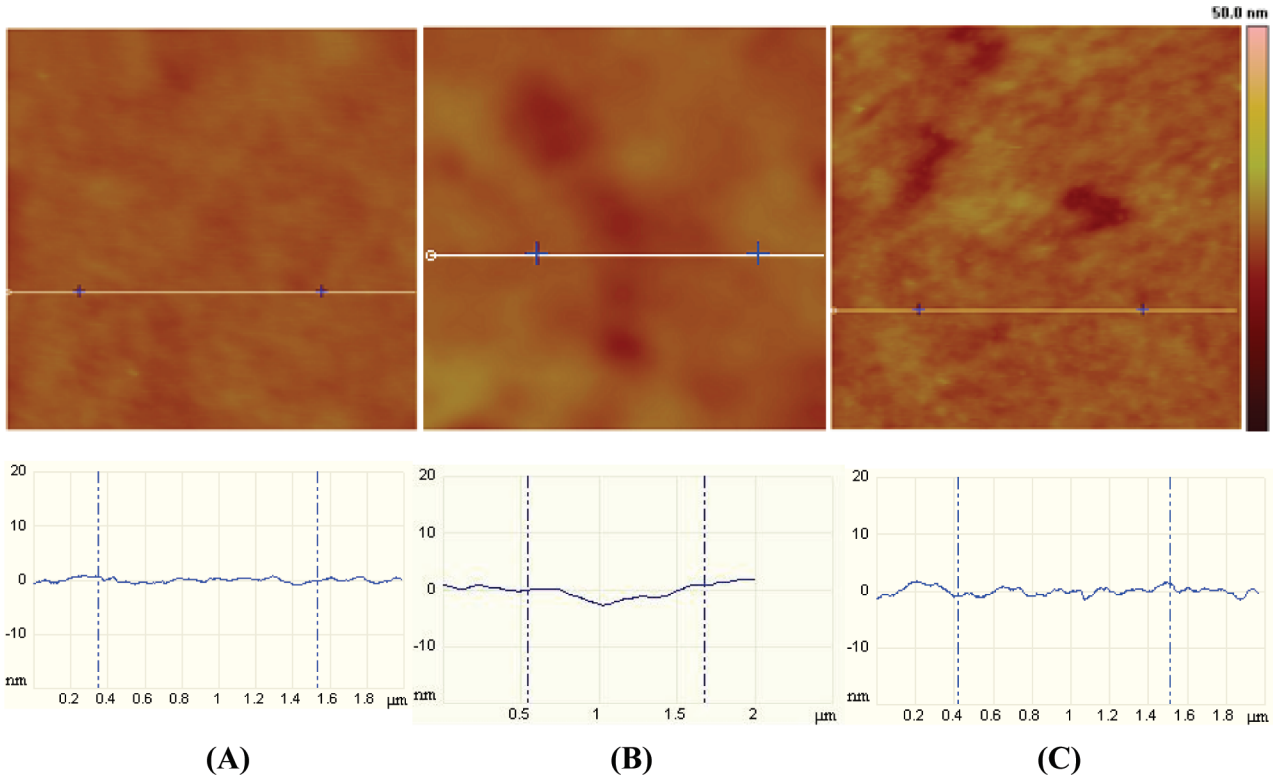

Figure 5. AFM topographic images (scan area: 2 × 2 μm^2) and the corresponding cross section of glycopolymer brushes containing different carbohydrate units: (A) PAAEM brush (38.4 nm), (B) PAAEGal brush (39.5 nm), and (C) PAAEGlc brush (38.7 nm).

The broad peak centered at 3334 cm^{-1} is assigned to the OH stretching vibration. The peak at 2929 cm^{-1} is due to the C−H asymmetric vibration mode of the $-CH_2-$ groups. AFM topographical images (Figure 5) showed that the glycopolymer grafted surface is relatively smooth. The surface roughness values for the PAAEM, PAAEGal, and PAAEGlc brushes are about 0.72, 0.9, and 1.4 nm, respectively.

Nonfouling Properties: A Proof-of-Concept Study. We performed a preliminary study to understand the nonbiofouling properties of new glycopolymer brushes containing different carbohydrate units. The ability to resist nonspecific protein adsorption by these surfaces was measured by fluorescence microscopy and ellipsometry. Samples having similar dry thickness and graft densities were used for the measurements. Two proteins, FITC labeled-albumin and Alex Fluor594 labeled Fb, were used in our experiments. Albumin is the most abundant protein in the circulatory system (~65%) and contributes 80% to colloid osmotic blood pressure. Fb is a large, blood plasma protein that strongly adsorbs to hydrophobic surfaces and is commonly used as a model for sticky serum proteins.

a. Effect of Carbohydrate Units. The thicknesses of PAAEM, PAAEGal, and PAAEGlc brushes did not show any noticeable change after incubation with BSA and Fb solution for 1 h (Figures 6A and 7A). The fluorescence intensities of the glycopolymer brushes after protein incubation were also compared with that of initiator-modified silicon wafer. The glycopolymer brushes containing mannose, galactose, and glucose significantly reduced the BSA adsorption, as evident from 149-, 172-, and 500-fold reduction in fluorescence intensity compared with the initiator-modified surface (Figure 6C). The Fb adsorptions were reduced by 52, 115 and 135-fold for the PAAEM, PAAEGal, and PAAEGlc brushes, respectively, (Figure 7C) compared with the initiator-modified surface. In the case of glycopolymer layer (PAAEM*) prepared from acetate-protected monomer, followed by deprotection, the reduction in the fluorescence intensity was only 2.4-fold. The large difference in reduction of protein adsorption again highlights the importance of preparation of glycopolymer brushes from unprotected monomer directly. The large reduction in protein adsorption brought by PAAEM, PAAEGla, and PAAEGlc brushes prepared from deprotected monomer directly may be due to (i) highly hydrophilic nature of brushes originated from carbohydrate residues possessing hydrogen-donating abilities,[65−68] (ii) entropic repulsion brought by the highly stretched chains in brushes,[69−71] and (iii) the chemical nature of carbohydrate units.[72,73] It is also shown from the nonspecific protein adsorption study that the PAAEGlc brushes (containing glucose units) showed better performance against BSA and Fb adsorption than the PAAEM and PAAEGla brushes (containing mannose and galactose units, respectively). The reason for the difference in nonbiofouling property is not clear at this time and is under investigation. The differences in the 3D arrangement of the hydroxyl groups of the carbohydrate units in the glycopolymer layer may disrupt the structural and dynamic properties of water layer bond to this layer through the hydrogen-bonding interaction.[73] Because protein-resistant properties of the hydrated brush surface are originated from the repulsive forces between the hydration layer and protein, any differences in the structural and dynamic properties of the water layer will bring a difference in the protein adsorption characteristics.[65,73]

b. Effect of Carbohydrate Structure. We compared the protein-resistant properties of PAAEGlc brushes with other glucose contain polymer brushes reported in the literature[28,35] (Figures 6B,D and 7B,D). PGAMA brushes, containing glucose in a linear structure (Scheme 4), showed similar abilities to that of PAAEGlc brushes against BSA and Fb adsorption, that is, 200- and 172-fold reduction, respectively, in comparison with initiator-modified layer. PMAGlc brushes, in which hydroxyl

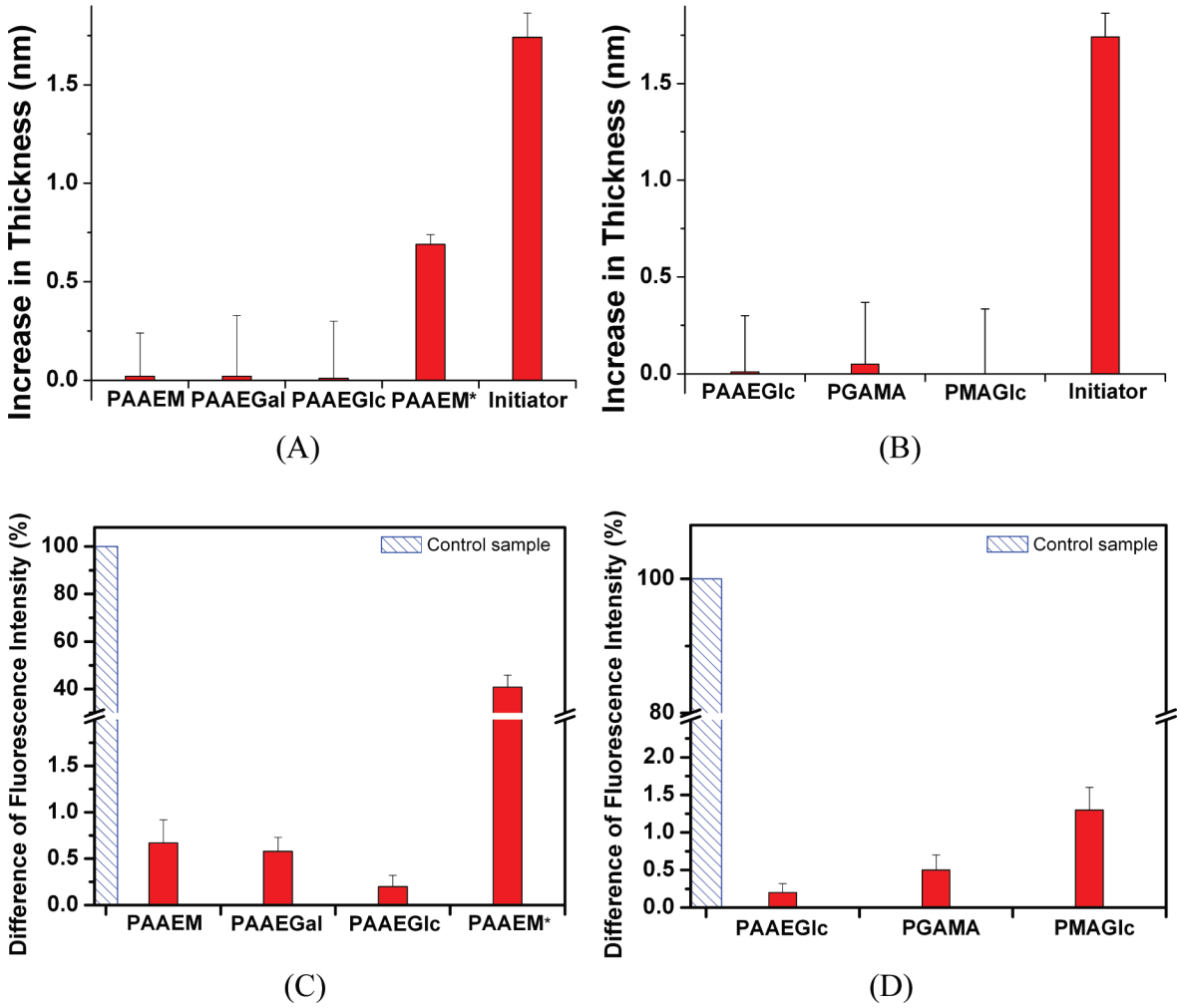

Figure 6. Comparison of nonspecific interaction of BSA: The increase in thicknesses of glycopolymer brushes containing (A) different carbohydrate units and (B) glucose units with different structures after BSA adsorption. (C) Fluorescence intensity reduction brought by glycopolymer brushes containing (A) different carbohydrate units and (D) glucose units with different structures after incubating with fluorescently labeled BSA. Initiator-modified silicon wafer was set as the control sample. PAAEM*: poly(2′-acrylamidoethyl-α-D-mannopyranoside) brushes prepared by polymerizing acetate protected monomer and followed by hydrolysis for 22 h. The original thicknesses for PAAEM, PAAEGla, PAAEGlc, PAAEM*, PGAMA, and PMAGlc before BSA adsorption are 38.4 ± 0.4, 39.6 ± 0.3, 38.8 ± 0.8, 5.5 ± 0.1, 37.2 ± 0.2, and 29.9 ± 0.2 nm, respectively. The grafting densities for PAAEM, PAAEGla, PAAEGlc, PAAEM*, PGAMA, and PMAGlc brushes are 0.16, 0.12, 0.12, 0.24, 0.3, and 0.25 chains/nm^2, respectively.

Scheme 4. Chemical Structures of (A) Poly(2′-acrylamidoethyl-β-D-glucopyranoside) brushes, (B) Poly(D-gluconamidoethyl methacrylate) (PGAMA),[35] and (C) Poly(3-*O*-methacryloyl-D-glucofuranose) (PMAGlc) Brushes[28]

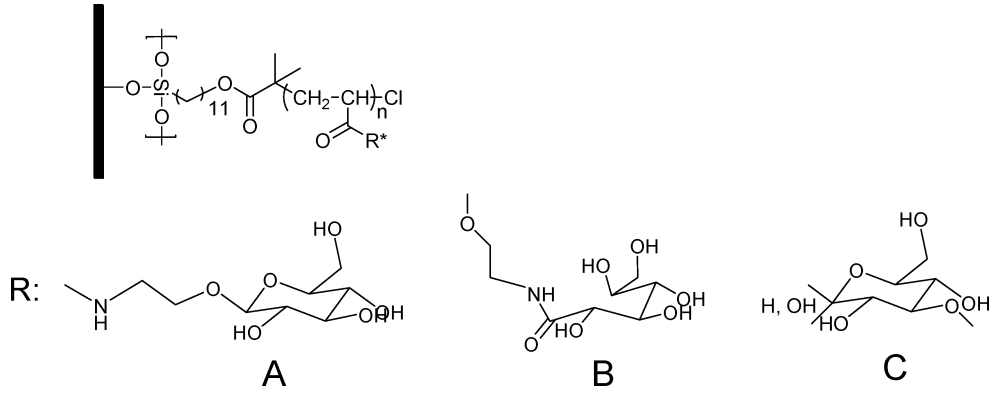

groups at position 3 of the pyranose ring in the glucose structure (Scheme 4) have been modified, gave a reduction of 77- and 3-fold against BSA and Fb adsorption, respectively. The relatively small reduction brought by the PMAGlc brushes maybe related to the incomplete deprotection within the brushes. The large difference in Fb adsorption between the PMAGlc and other brushes again highlights the importance of preparation of glycopolymer brushes from unprotected monomer directly.

Specific Interaction with Protein: a Proof-of-Concept Study. Con A, is a 26 000 MW monomer that exists as a dimer at low (<5.5) pH and as a tetramer at high (>7) pH.[74] Each

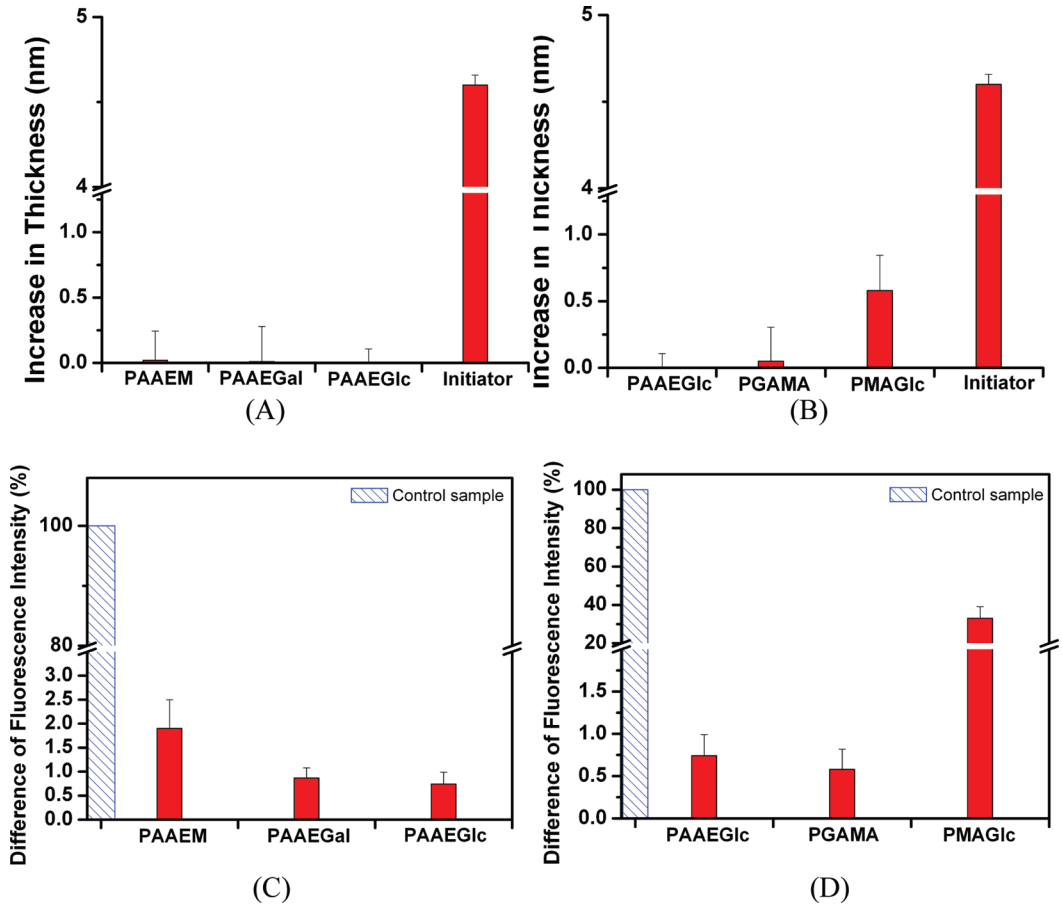

Figure 7. Comparison of nonspecific interaction of fibrinogen: The increase in thicknesses of glycopolymer brushes containing (A) different carbohydrate units and (B) glucose units with different structures after fibrinogen adsorption. (C) Fluorescence intensity reduction brought by glycopolymer brushes containing (A) different carbohydrate units and (D) glucose units with different structures after incubating with fluorescently labeled fibrinogen. Initiator-modified silicon wafer was set as the control sample. The original thicknesses for PAAEM, PAAEGla, PAAEGlc, PGAMA, and PMAGlc before BSA adsorption are 39.3 ± 0.2, 40.1 ± 0.2, 39.2 ± 0.5, 37.2 ± 0.2, and 29.9 ± 0.2 nm, respectively. The grafting densities for PAAEM, PAAEGla, PAAEGlc, PGAMA, and PMAGlc brushes are 0.16, 0.12, 0.12, 0.3, and 0.25 chains/nm^2, respectively.

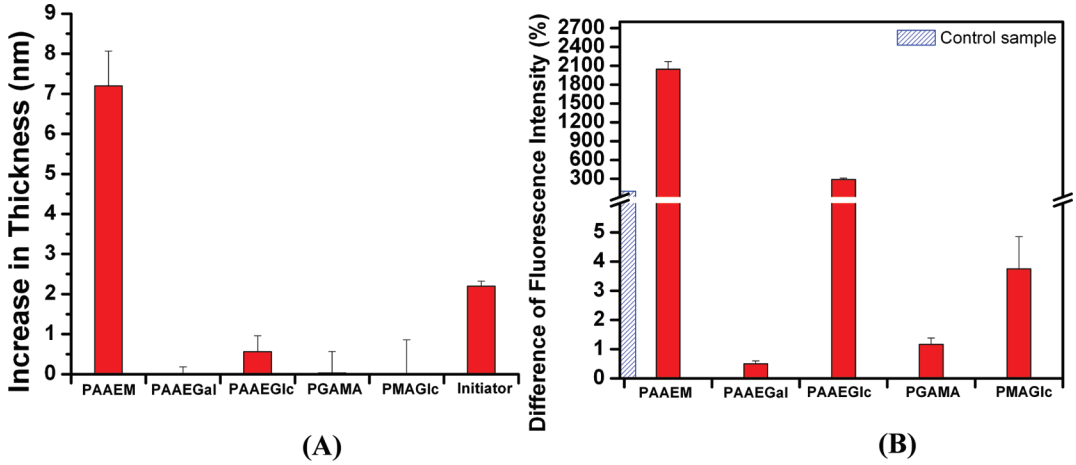

Figure 8. Comparison of specific interaction of Con A: (A) Increase in thicknesses of glycopolymer after Con A adsorption and (B) fluorescence intensity reduction brought by glycopolymer brushes containing different carbohydrate units after incubating with fluorescently labeled Con A. Initiator-modified silicon wafer was set as the control sample. The original thicknesses for PAAEM, PAAEGla, PAAEGlc, PGAMA, and PMAGlc before Con A adsorption are 41.5 ± 0.8, 42.1 ± 0.5, 42.5 ± 0.3, 37.6 ± 0.4, and 30.5 ± 0.5 nm, respectively. The grafting densities for PAAEM, PAAEGla, PAAEGlc, PGAMA, and PMAGlc brushes are 0.16, 0.12, 0.12, 0.3, and 0.25 chains/nm^2, respectively.

subunit contains a binding site that binds ligands with unmodified hydroxyls of the carbohydrate units.

a. Effect of Different Carbohydrate Units. Figure 8 shows that Con A has a specific interaction with glycopolymer brushes containing mannose and glucose units, not galactose units. After incubation with Con A, the thickness of brush layer increased by 7.2 and 0.6 nm, respectively, for PAAEM brushes and PAAEGlc brushes. The fluorescence intensities increased by 20.5- and 2.9-fold compared with control samples, respectively. It has been reported that D-mannopyrannoside shows approximately four times affinity to Con A compared with D-glucopyrannoside in the case of monovalent binding.[75] The

enhanced difference in specific interaction with glycopolymer brushes may also be brought by the multivalent binding due to the "glyco-cluster" effect. In summary, our results show that PAAEM and PAAEGlc brushes prevented nonspecific interactions and preserved the specific interaction with Con A as well.

b. Effect of Modification of Carbohydrate Structure. To illustrate the effect of carbohydrate structure on the specific interaction with lectins, we compared the ConA interaction profiles of PAAEGlc with PGAMA[35] and PMAGlc[28] brushes (Figure 8). In comparison with PAAEGlc brushes, PGAMA and PMAGlc showed very weak interaction with Con A. As previously discussed, the glucose unit in the PGAMA has a linear glucose structure, which is quite different from its natural pyranose form, not able to interact with Con A specifically. In the case of PMAGlc brushes, although the carbohydrate units in PMAGlc brushes are in the pyranose form, the hydroxyl group at position 3 has been modified. The modification hindered the specific protein interaction. Because PAAEGlc brushes have sugar units in pyranose form and the sugar unit is not modified, they gave much better interaction with Con A compared with PGAMA or PMAGlc. The residual adsorption shown by these surfaces may be due to the nonspecific interactions. This is consistent with the report by Goldstein et al. that a monosaccharide is required to have D-manno- or D-glucopyranose configuration with unmodified hydroxyl groups at the C-3, C-4, and C-6 positions to bind strongly to ConA.[76] Our results highlight the importance of natural sugar structure for retaining the specific protein interactions.

Conclusions

Three novel monomers containing mannose, galactose, and glucose in the pyranose form were synthesized using the protection−deprotection strategy. Homoglycopolymer brushes were prepared by SI-ATRP of these newly synthesized monomers. The utilization of $CuCl/CuCl_2/Me_6TREN$ as the catalyst and H_2O as the solvent gave better control of brush growth compared with other systems studied. The molecular weight, thickness, and graft density were changed by modifying the experimental parameters. The kinetics study showed that the initial rate of the polymerization in solution and growth of polymer brushes were very fast. The synthesized glycopolymer surfaces were highly hydrophilic compared with the structures available in the literature. These newly synthesized surfaces showed ultralow protein adsorption against BSA and fibronogen. The glycopolymer brush containing glucose residues showed better performance against protein adsorption compared with the brushes containing mannose and galactose units. The specific protein interactions studies with Con A showed the importance of the preserving carbohydrate structure in its natural form in the design of surface for enhancing the specific protein interactions. Our brushes virtually eliminated nonspecific protein interactions but preserved the specific protein interactions.

Acknowledgment. We acknowledge the funding provided by the Canadian Diabetes Association, NSERC, and CIHR. The LMB Macromolecular Hub at the UBC Centre for Blood Research was funded by CFI and MSFHR. K.Y. is a recipient of a CIHR/Canadian Blood Services (CBS) postdoctoral fellowship in Transfusion Science. K.Y. also acknowledges a postdoctoral fellowship from the Strategic Training Program in Transfusion Science at the Centre for Blood Research supported by CIHR and Heart and Stroke Foundation of Canada. J.N.K. is a recipient of a CIHR/CBS new investigator in Transfusion Science.

Supporting Information Available. Experimental details and characterization of compounds containing galactose and glucose units, XPS data of surface initiator, ^1H NMR spectra of poly(2′-acrylamido-2,3,4,6-tetra-*O*-acetyl-α-D-mannopyranoside) before and after deprotection, details of deprotection of poly(2′-acrylamido-2,3,4,6-tetra-*O*-acetyl-α-D-mannopyranoside) brush, GPC traces of glycopolymers, and so on. This material is available free of charge via the Internet at http://pubs.acs.org.

References and Notes

(1) Lis, H.; Sharon, N. *Chem. Rev.* **1998**, *98*, 637–674.
(2) Flitsch, S. L.; Ulijn, R. V. *Nature* **2003**, *421*, 219–220.
(3) Kitov, P. I.; Sadowska, J. M.; Mulvey, G.; Armstrong, G. D.; Ling, H.; Pannu, N. S.; Read, R. J.; Bundle, D. R. *Nature* **2000**, *403*, 669–672.
(4) Joo, K. L.; Mao, S.; Sun, C.; Gao, C.; Blixt, O.; Arrues, S.; Hom, L. G.; Kaufmann, G. F.; Hofmann, T. Z.; Coyle, A. R.; Paulson, J.; Felding-Habermann, B.; Janda, K. D. *J. Am. Chem. Soc.* **2002**, *124*, 12439–12446.
(5) Foa, C.; Soler, M.; Benoliel, A. M.; Bongrand, P. *J. Mater. Sci: Mater. Med.* **1996**, *7*, 141–148.
(6) Dwek, R. A. *Chem. Rev.* **1996**, *96*, 683–720.
(7) Bertozzi, C. R.; Kiessling, L. L. *Science* **2001**, *291*, 2357–2364.
(8) Alberts, B.; Bray, D.; Lewis, J.; Raff, M.; Roberts, K.; Watson, J. *Molecular Biology of the Cell*, 3rd ed.; Garland Science: New York, 1994; pp 477−506.
(9) Wang, D.; Liu, S.; Trummer, B.; Deng, C.; Wang, A. *Nat. Biotechnol.* **2002**, *20*, 275–281.
(10) Fukui, S.; Feizi, T.; Galustian, C.; Lawson, A.; Chai, W. *Nat. Biotechnol.* **2002**, *20*, 1011–1017.
(11) Holland, N. B.; Qiu, Y.; Ruegsegger, M.; Marchant, R. E. *Nature* **1998**, *392*, 799–801.
(12) Sen Gupta, A.; Wang, S.; Link, E.; Anderson, E. H.; Hofmann, C.; Lewandowski, J.; Kottke-Marchant, K.; Marchant, R. E. *Biomaterials* **2006**, *27*, 3084–3095.
(13) Zhu, J. M.; Marchant, R. E. *Biomacromolecules* **2006**, *7*, 1036–1041.
(14) Bosker, W. T. E.; Patzsch, K.; Stuart, M. A. C.; Norde, W. *Soft Matter* **2007**, *3*, 754–762.
(15) Smith, E. A.; Thomas, W. D.; Kiessling, L. L.; Corn, R. M. *J. Am. Chem. Soc.* **2003**, *125*, 6140–6148.
(16) Hederos, M.; Konradsson, P.; Liedberg, B. *Langmuir* **2005**, *21*, 2971–2980.
(17) Stevens, J.; Blixt, O.; Glaser, L.; Taubenberger, P. P.; Paulson, J. C.; Wilson, I. A. *J. Mol. Biol.* **2006**, *355*, 1143–1155.
(18) Cao, X.; Pettit, M. E.; Conlan, S. L.; Wagner, W.; Ho, A. D.; Clare, A. S.; Callow, J. A.; Callow, M. E.; Grunze, M.; Rosenhahn, A. *Biomacromolecules* **2009**, *10*, 907–915.
(19) De Smet, L. C. P. M.; Stork, G. A.; Hurenkamp, G. H. F.; Sun, Q. Y.; Huseyin, T.; Vronen, P. J. E.; Sieval, A. B.; Wright, A.; Visser, G. M.; Zulihoff, H.; Sudholter, E. J. R. *J. Am. Chem. Soc.* **2003**, *125*, 13916–13917.
(20) Liang, P.-H.; Wang, S.-K.; Wong, C.-H. *J. Am. Chem. Soc.* **2007**, *129*, 11177–11184.
(21) Huang, C. H.; Thayer, D. A.; Chang, A. Y.; Best, M. D.; Hoffmann, J.; Head, S.; Wong, C.-H. *Proc. Natl. Acad. Sci. U.S.A.* **2006**, *103*, 15–20.
(22) Zhang, Y.; Luo, S.; Tang, Y.; Yu, L.; Hou, K.-Y.; Cheng, J.-P.; Zeng, X.; Wang, P. G. *Anal. Chem.* **2006**, *78*, 2001–2008.
(23) Sun, X.-L.; Stabler, C. L.; Cazalis, C. S.; Chaikof, E. L. *Bioconjugate Chem.* **2006**, *17*, 52–57.
(24) Harris, L. G.; Schofield, W. C. E.; Doores, K. J.; Davis, B. G.; Badyal, J. P. S. *J. Am. Chem. Soc.* **2009**, *131*, 7755–7761.
(25) Mandal, D. K.; Kishore, N.; Brewer, C. F. *Biochemistry* **1994**, *33*, 1149–1156.
(26) Schwarz, F. P.; Puri, K. D.; Bhat, R. G.; Surolia, A. *J. Biol. Chem.* **1993**, *268*, 7668–7677.
(27) Ohno, K.; Tsujii, Y.; Fukuda, T. *J. Polym. Sci., Part A: Polym. Chem.* **1998**, *36*, 2473–2481.
(28) Ejaz, M.; Ohno, K.; Tsujii, Y.; Fukuda, T. *Macromolecules* **2000**, *33*, 2870–2874.
(29) Gao, C.; Muthukrishnan, S.; Li, W. W.; Yuan, J. Y.; Xu, Y. Y.; Müller, A. H. E. *Macromolecules* **2007**, *40*, 1803–1815.
(30) Muthukrishnan, S.; Erhard, D. P.; Mori, H.; Müller, A. H. E. *Macromolecules* **2006**, *39*, 2743–2750.
(31) Narain, R.; Armes, S. P. *Biomacromolecules* **2003**, *4*, 1746–1758.

(32) Yang, Q.; Tian, J.; Hu, M. X.; Xu, Z. K. *Langmuir* **2007**, *23*, 6684–6690.
(33) Yang, Q.; Xu, Z. K.; Dai, Z. W.; Wang, J. L.; Ulbricht, M. *Chem. Mater.* **2005**, *17*, 3050–3058.
(34) Raynor, J. E.; Petrie, T. A.; Fears, K. P.; Latour, R. A.; García, A. J.; Collard, D. M. *Biomacromolecules* **2009**, *10*, 748–755.
(35) Yang, Q.; Kaul, C.; Ulbricht, M. *Langmuir* **2010**, *26*, 5746−5752.
(36) Varki, A. In *Essentials of Glycobiology*, 1st ed.; Varki, A., Cummings, R. D., Esko, J. D., Freeze, H. H. , et al., Eds.; Cold Spring Harbor Laboratory Press: Plainview, NY, 1999; p 4.
(37) Yang, Q.; Wu, J.; Li, J.-J.; Hu, M.-X.; Xu, Z.-K. *Macromol. Rapid Commun.* **2006**, *27*, 1942–1948.
(38) Mateescu, A.; Ye, J.; Narain, R.; Vamvakaki, M. *Soft Matter* **2009**, *5*, 1621–1629.
(39) Dowlut, M.; Hall, D. G.; Hindsgaul, O. *J. Org. Chem.* **2005**, *70*, 9809–9813.
(40) Ciampolini, M.; Nardi, N. *Inorg. Chem.* **1966**, *5*, 41–44.
(41) Matyjaszewski, K.; Miller, P. J.; Shukla, N.; Immaraporn, B.; Gelman, A.; Luokala, B. B.; Siclovan, T. M.; Kickelbick, G.; Vallant, T.; Hoffmann, H.; Pakula, T. *Macromolecules* **1999**, *32*, 8716–8724.
(42) Yeh, P. Y.; Kizhakkedathu, J. N.; Madden, J. D.; Chiao, M. *Colloids Surf., B* **2007**, *59*, 67–73.
(43) Yeh, P. J.; Kainthan, R.; Zou, Y.; Chiao, M.; Kizhakkedathu, J. N. *Langmuir* **2008**, *24*, 4907–4916.
(44) Murahashi, S.; Yoshimura, N.; Tsumiyama, T.; Kojima, T. *J. Am. Chem. Soc.* **1983**, *105*, 5002–5011.
(45) Tsuji, Y.; Shida, J.; Takeuchi, R.; Watanabe, Y. *Chem. Lett.* **1984**, *13*, 889–890.
(46) Brittain, W. J.; Boyes, S. G.; Granville, A. M.; Baum, M.; Mirous, B. K.; Akgun, B.; Zhao, B.; Blickle, C.; Foster, M. D. *Adv. Polym. Sci.* **2006**, *198*, 125–147.
(47) Teodorescu, M.; Matyjaszewski, K. *Macromolecules* **1999**, *32*, 4826–4831.
(48) Tsarevsky, N. V.; Pintauer, T.; Matyjaszewski, K. *Macromolecules* **2004**, *37*, 9768–9778.
(49) Matyjaszewski, K.; Shipp, D. A.; Wang, J.-L.; Grimaud, T.; Patten, T. E. *Macromolecules* **1998**, *31*, 6836–6840.
(50) Kizhakkedathu, J. N.; Brooks, D. E. *Macromolecules* **2003**, *36*, 591–598.
(51) Kizhakkedathu, J. N.; Norris-Jones, R.; Brooks, D. E. *Macromolecules* **2004**, *37*, 734–743.
(52) Neugebauer, D.; Matyjaszewski, K. *Macromolecules* **2003**, *36*, 2598–2603.
(53) Xia, Y.; Yin, X.; Burke, N. A. D.; Stover, H. A. H. *Macromolecules* **2005**, *38*, 5937–5943.
(54) Sankhe, A. Y.; Husson, S. M.; Kilbey, S. M., II. *Macromolecules* **2006**, *39*, 1376–1383.
(55) Wei, X.; Li, X.; Husson, S. M. *Biomacromolecules* **2005**, *6*, 1113–1121.
(56) Zou, Y.; Kizhakkedathu, J. N.; Brooks, D. E. *Macromolecules* **2009**, *42*, 3258–3268.
(57) Zou, Y.; Rossi, N. A. A.; Kizhakkedathu, J. N.; Brooks, D. E. *Macromolecules* **2009**, *42*, 4817–4828.
(58) Fan, X.; Lin, L.; Dalsin, J. L.; Messersmith, P. B. *J. Am. Chem. Soc.* **2005**, *127*, 15843–15847.
(59) Ma, H.; Hyun, J.; Stiller, P.; Chilkoti, A. *Adv. Mater.* **2004**, *16*, 338–341.
(60) Huang, W.; Kim, J.-B.; Bruening, M. L.; Baker, G. L. *Macromolecules* **2002**, *35*, 1175–1179.
(61) Jones, D. M.; Huck, W. T. S. *Adv. Mater.* **2001**, *13*, 1256–1259.
(62) Yu, W. H.; Kang, E. T.; Neoh, K. G. *Langmuir* **2004**, *20*, 8294–8300.
(63) Perrier, S.; Haddleton, D. M. *Macromol. Symp.* **2002**, *182*, 261–272.
(64) Haddleton, D. M.; Perrier, S.; Bon, S. A. F. *Macromolecules* **2000**, *33*, 8246–8251.
(65) Herrwerth, S.; Eck, W.; Reinhardt, S.; Grunze, M. *J. Am. Chem. Soc.* **2003**, *125*, 9359–9366.
(66) Schilp, S.; Rosenhahn, A.; Pettitt, M. E.; Bowen, J.; Callow, M. E.; Callow, J. A.; Grunze, M. *Langmuir* **2009**, *25*, 10077–10082.
(67) Hucknall, A.; Rangarajan, S.; Chilkoti, A. *Adv. Mater.* **2009**, *21*, 2441–2446.
(68) Senaratne, W.; Andruzzi, L.; Ober, C. K. *Biomacromolecules* **2005**, *6*, 2427–2448.
(69) Singh, N.; Cui, X.; Boland, T.; Husson, S. M. *Biomaterials* **2007**, *28*, 763–771.
(70) Feng, W.; Brash, J.; Zhu, S. *Biomaterials* **2006**, *27*, 847–855.
(71) Kizhakkedathu, J. N.; Janzen, J.; Le, Y.; Kainthan, R. K.; Brooks, D. E. *Langmuir* **2009**, *25*, 3794–3801.
(72) Luk, Y.-Y.; Kato, M.; Mrksich, M. *Langmuir* **2000**, *16*, 9604–9608.
(73) Hower, J. C.; He, Y.; Bernards, M. T.; Jiang, S. *J. Chem. Phys.* **2006**, *125*, 214704.
(74) Weatherman, R. V.; Mortell, K. I.; Chervenak, M.; Kiessling, L. L.; Toone, E. J. *Biochemistry* **1996**, *35*, 3619–3625.
(75) Schwarz, F. P.; Puri, K. D.; Bhat, R. G.; Surolia, A. *J. Biol. Chem.* **1993**, *268*, 7668–7677.
(76) Goldstein, I. J.; Hollerman, C. E.; Smith, E. E. *Biochemistry* **1965**, *4*, 876–883.

BM100882Q